

**CBPF - CENTRO BRASILEIRO DE PESQUISAS FÍSICAS**

**Rio de Janeiro**

**Notas de Física**

**CBPF-NF-048/01**

**August 2001**

**Photofissility of Actinide Nuclei at Intermediate Energies**

A. Deppman, O.A.P. Tavares, S.B. Duarte, E.C. de Oliveira, J.D.T. Arruda-Neto,  
S.R. de Pina, V.P. Likhachev, O. Rodriguez, J. Mesa and M. Gonçalves

CERN LIBRARIES, GENEVA



CMF00038415

11-2292 855

## Photofissility of Actinide Nuclei at Intermediate Energies

A.Deppman<sup>a1</sup>, O.A.P.Tavares<sup>a</sup>, S.B.Duarte<sup>a</sup>, E.C. de Oliveira<sup>a</sup>, J.D.T. Arruda-Neto<sup>b,c</sup>,  
S.R. de Pina<sup>b</sup>, V.P. Likhachev<sup>b</sup>, O. Rodriguez<sup>b,d</sup>, J. Mesa<sup>b</sup>, and M. Gonçalves<sup>e2</sup>.

<sup>a)</sup>Centro Brasileiro de Pesquisas Físicas -CBPF/MCT

22290-180 Rio de Janeiro, Brazil

<sup>b)</sup>Instituto de Física da Universidade de São Paulo

P.O.Box 66318 - CEP 05315-970

São Paulo, Brazil

<sup>c)</sup>Universidade de Santo Amaro - UNISA

São Paulo, Brazil

<sup>d)</sup>Instituto Superior de Ciencias y Tecnología Nucleares - ISCTN

A.P. 6163 La Habana, Cuba

<sup>e)</sup>Instituto de Radioproteção e Dosimetria - IRD/CNEN

22780-160 Rio de Janeiro, Brazil

August 2001

### Abstract

We analyze the recent experimental data on photofissility for  $^{237}\text{Np}$ ,  $^{238}\text{U}$ , and  $^{232}\text{Th}$  at incident photon energies above  $200\text{MeV}$ . For this analysis, we developed a Monte Carlo algorithm for the nuclear evaporation process in photonuclear reactions. This code is used in association with the multi-collisional model for the photon-induced intranuclear cascade process. Our results show a good quantitative and qualitative agreement with the experimental data. It is shown that the emission of protons and alpha particles at the evaporation stage is an important component for the non-saturation of the actinides photofissility up to, at least,  $1\text{GeV}$ .

PACS25.85.Jg, 25.20.-x, 25.85.-w

**Key-words:** Photonuclear reactions; Photofission; Photofissility

It has been widely believed that the fissility ( $W$ ) of actinide nuclei should saturate at 100% for energies above  $\sim 100\text{MeV}$ [1, 2, 3, 4]. Such a possibility is so appealing and convincing that several groups have been proposing research projects devoted to the systematic investigation of the photoabsorption process at intermediate and high energies. In fact, since  $W = 1$ , photofission cross section measurements would propitiate a good evaluation for the total nuclear photoabsorption cross section [4, 5, 6], and this would configurate the easiest and most direct method of photoabsorption cross section measurement for the heavy nuclei. However, as pointed out elsewhere[5, 6, 7], the total nuclear photoabsorption cross section is an important and interesting source of information on the role played by the nuclear medium in the intrinsic properties and interaction aspects of the nucleons, as well as on the earlier stages of the “shadowing” effect, a manifestation of the hadronic nature of the photon.

The first disturbance in this optimistic scenario came, however, with the experimental results for the photofissility of  $^{232}\text{Th}$ . It was found that  $W$  is  $\sim 60\%$  to  $\sim 80\%$  of that for  $^{238}\text{U}$  in the energy interval  $200 - 1200\text{MeV}$ [4]. Because of some precedents associated with the photoprocess in  $^{232}\text{Th}$ , as the well-known “thorium anomalies” manifesting at low and intermediate energies[8, 9, 10], it could be conjectured that the non-saturation of the  $^{232}\text{Th}$  photofissility, at energies as high as  $1.2\text{GeV}$ , is another sort of unexplained anomaly exhibited by this nuclide. In this regard, a phenomenological description of the photofissility[10], suggested that the non-saturation of photofissility in  $^{232}\text{Th}$  could be a consequence of its higher nuclear transparency comparatively to that of  $^{238}\text{U}$ , and a model based on the nuclear structure was proposed in Ref. [11] to explain these photofissility results. The second difficulty came from photofission results for  $^{237}\text{Np}$  reported by the Novosibirsk group in the early nineties[3]. Quite disturbing at that time, the results revealed a photofissility for  $^{237}\text{Np}$ , in the energy interval  $60 - 240\text{MeV}$ , nearly 30% higher than that for  $^{238}\text{U}$ . These results were confirmed quite recently by Sanabria and collaborators[12], in a photofission experiment carried out in Saskatoon. No convincing explanation has so far been presented for these findings. Finally, in a recent experiment performed at the Photon Tagging Facility in Hall B at the Thomas Jefferson Laboratory, Cetina et al.[13] thoroughly demonstrated that the photofission cross section for  $^{238}\text{U}$  is about 80% of that for  $^{237}\text{Np}$  up to  $\sim 4\text{GeV}$ . Again, neither qualitative nor quantitative explanation has been proposed. These findings claim for a convincing explanation given

their several implications on nuclear structure aspects[1, 4, 11], on compound nucleus formation mechanisms[10], and on the potentialities of the fission channel as a probe to infer new nuclear reactions characteristics[4, 5].

In this letter we present for the first time a complete and detailed calculation of the photofissility for actinide nuclei. This is achieved by using a combination of the multicollisional Monte Carlo calculation (MCMC - described in Ref. [14]) for the photon-induced intranuclear cascade process, and a new Monte Carlo algorithm developed by us for the evaporation-fission process, which includes not only the neutron evaporation *vs.* fission competition, but also takes into account the evaporation of protons and alpha particles. We have applied these calculational procedures to obtain the photofissility of  $^{237}\text{Np}$ ,  $^{238}\text{U}$  and  $^{232}\text{Th}$ . As discussed below, our results provide a good description of the experimental absolute and relative photofissilities from  $0.2\text{GeV}$  to  $1\text{GeV}$ . We did not extend the calculation above  $1\text{GeV}$  because a significant shadowing effect takes place at higher energies, starting below  $1.5\text{GeV}$ [13, 15], and this effect is not yet included in our intranuclear cascade calculation.

The MCMC method propitiates a more realistic description of the intranuclear cascade process, comparatively to the traditional methods[16, 17], since it gives a time-ordered evolution of the cascade by taking into account the nucleus configuration at each instant of time. The evaluation of the collisional probabilities among the nucleons, as well as the secondaries arising from these collisions, is carried out[14]. Such a realistic description results in a higher multiplicity of protons and neutrons leading, thus, to the formation of less massive compound nuclei as compared with those coming from traditional intranuclear cascade calculations. This aspect is the key to the photofissility non-saturation clue, because lighter nuclei have lower fission probabilities. We were, then, motivated to develop an algorithm for the evaporation process, which is a complement to the multicollisional algorithm. With the former we calculate the evaporation-fission competition taking place in the compound nuclei, which is obtained from the latter. The compound nucleus,  $(A_c, Z_c)$ , have excitation energy,  $E_c$ , which is in accordance with the results of a previous analysis on the subject [10].

The probability for the emission of a particle  $j$  with kinetic energy between  $E_k$  and  $E_k + dE_k$  is calculated according to the Weisskopf's statistical model[18] as,

$$P_j(E_k) dE_k = \gamma_j \sigma_j E_k \left( \frac{\rho_f}{\rho_i} \right) dE_k, \quad (1)$$

where  $\sigma_j$  is the nuclear capture cross section for particle  $j$  by the final nucleus,  $\gamma_j = \frac{gm}{(\pi^2 \hbar^3)}$ , where  $g$  denotes the number of spin states, and  $m$  is the particle mass. The level density for the initial and final nuclei,  $\rho_i$  and  $\rho_f$ , respectively, are calculated from the Fermi gas expression

$$\rho(E_j^*) = \exp\left(2(aE_j^*)^{\frac{1}{2}}\right), \quad (2)$$

where  $a$  is the level density parameter, and

$$E_j^* = E^* - (B_j + V_j). \quad (3)$$

Here,  $E^*$  is the nuclear excitation energy in the initial state,  $B_j$  is the particle separation energy, and  $V_j$  is the Coulomb potential barrier corrected for the nuclear temperature,  $\tau$ , defined as  $E^* = a\tau^2$ .

The particle emission width is calculated as

$$\Gamma_j = \int_0^{E_j^*} P_j(E_k) dE_k. \quad (4)$$

From this general equation, we obtain the  $k$ -particle emission probability relatively to  $j$ -particle emission, that is

$$\frac{\Gamma_k}{\Gamma_j} = \left( \frac{\gamma_k}{\gamma_j} \right) \left( \frac{E_k^*}{E_j^*} \right) \left( \frac{a_j}{a_k} \right) \exp\left\{2\left[(a_k E_k^*)^{\frac{1}{2}} - (a_j E_j^*)^{\frac{1}{2}}\right]\right\}. \quad (5)$$

The level density parameter for neutron emission is[19]

$$a_n = 0.134A - 1.21 \cdot 10^{-4} A^2 \text{MeV}^{-1}, \quad (6)$$

and for all other particle emission this quantity is related to  $a_n$  by

$$a_j = r_j a_n, \quad (7)$$

where  $r_j$  is an dimensionless constant.

The shell model corrections[20] are not taken into account, since they are small at intermediate excitation energies and are likely to cancel with each other on the average over all possible nuclei created during the reaction.

Using the fission width from the liquid drop model for fission by Bohr and Wheeler[21], and the neutron emission width from Weisskopf[18], we get[22]

$$\frac{\Gamma_f}{\Gamma_n} = K_f \exp \left\{ 2 \left[ (a_f E_f^*)^{\frac{1}{2}} - (a_n E_n^*)^{\frac{1}{2}} \right] \right\}, \quad (8)$$

where

$$K_f = K_0 a_n \frac{[2(a_f E_f^*)^{\frac{1}{2}} - 1]}{(4A^{\frac{2}{3}} a_f E_n^*)}, \quad (9)$$

and

$$E_f^* = E^* - B_f, \quad (10)$$

with  $K_0 = 14.39 \text{ MeV}$ . Here,  $B_f$  is the fission barrier height discussed below.

For proton emission we get

$$\frac{\Gamma_p}{\Gamma_n} = \left( \frac{E_p^*}{E_n^*} \right) \exp \left\{ 2 (a_n)^{\frac{1}{2}} \left[ (r_p E_p^*)^{\frac{1}{2}} - (E_n^*)^{\frac{1}{2}} \right] \right\}, \quad (11)$$

and for alpha particle emission

$$\frac{\Gamma_\alpha}{\Gamma_n} = \left( \frac{2E_\alpha^*}{E_n^*} \right) \exp \left\{ 2 (a_n)^{\frac{1}{2}} \left[ (r_\alpha E_\alpha^*)^{\frac{1}{2}} - (E_n^*)^{\frac{1}{2}} \right] \right\}. \quad (12)$$

The Coulomb potential[23] (see Eq. (3)) for proton is

$$V_p = C \frac{[K_p (Z-1) e^2]}{[r_0 (A-1)^{\frac{1}{3}} + R_p]}, \quad (13)$$

and for alpha particle it is

$$V_\alpha = C \frac{[2K_\alpha (Z-2) e^2]}{[r_0 (A-4)^{\frac{1}{3}} + R_\alpha]}, \quad (14)$$

where  $K_p = 0.70$  and  $K_\alpha = 0.83$  are the Coulomb barrier penetrabilities for protons and alpha particles, respectively,  $R_p = 1.14 \text{ fm}$  is the proton radius,  $R_\alpha = 2.16 \text{ fm}$  is the alpha particle radius,  $r_0 = 1.2 \text{ fm}$ , and

$$C = 1 - \frac{E^*}{B} \quad (15)$$

is the charged-particle Coulomb barrier correction due to the nuclear temperature [23], with  $B$  being the nuclear binding energy. In addition, according to Ref. [24], we use  $r_p = r_\alpha = 1$ .

The fission barrier is calculated by[20]

$$B_f = C(0.22(A-Z) - 1.40Z + 101.5) \text{ MeV}; \quad (16)$$

the neutron binding energy is given by[20]

$$B_n = (-0.16(A - Z) + 0.25Z + 5.6)MeV, \quad (17)$$

while the proton and alpha particle binding energies are calculated, respectively, through the expressions:

$$B_p = m_p + m(A - 1, Z - 1) - m(A, Z), \quad (18)$$

and

$$B_\alpha = m_\alpha + m(A - 4, Z - 2) - m(A, Z), \quad (19)$$

where  $m_p$  is the proton mass,  $m_\alpha$  is the alpha particle mass, and  $m(A, Z)$  is the nuclear mass calculated with the parameter values from Ref. [25].

The present Monte Carlo code for Evaporation-Fission (MCEF) calculates, at each step  $i$  of the evaporation process, the nuclear fission probability,  $F_i$ , defined as

$$F_i = \frac{\left(\frac{\Gamma_f}{\Gamma_n}\right)_i}{1 + \left(\frac{\Gamma_f}{\Gamma_n}\right)_i + \left(\frac{\Gamma_p}{\Gamma_n}\right)_i + \left(\frac{\Gamma_\alpha}{\Gamma_n}\right)_i}, \quad (20)$$

with the values  $\frac{\Gamma_f}{\Gamma_n}$ ,  $\frac{\Gamma_p}{\Gamma_n}$  and  $\frac{\Gamma_\alpha}{\Gamma_n}$  calculated by equations (8), (11) and (12), respectively. Then, the particle that will evaporate (neutron, proton or alpha particle) is chosen randomly, according to their relative branching ratio (see equation (5)). Once one of these particles is chosen, the mass and atomic numbers are recalculated by

$$A_{i+1} = A_i - \Delta A_i, \quad (21)$$

and

$$Z_{i+1} = Z_i - \Delta Z_i, \quad (22)$$

where  $\Delta A_i$ , and  $\Delta Z_i$ , are, respectively, the mass and atomic numbers of the ejected particle at the  $i^{th}$  step in the evaporation process. Also, the nuclear excitation energy is modified according to the expression

$$E_{i+1}^* = E_i^* - B_i - T_i, \quad (23)$$

where  $B_i$  and  $T_i$  are the separation and the asymptotic kinetic energies of the particle being ejected, respectively. For neutrons,  $T = 2MeV$ , for protons  $T = V_p$ , and for alpha particles  $T = V_\alpha$ .

Expression (23) ensures that the nuclear excitation energy will be, at each step in the evaporation chain, smaller than in the previous step. This process continues until the excitation energy available in the nucleus is not enough to emit any of the possible evaporating particles. At this point the evaporation process stops, and we can calculate the nuclear fissility by the expression

$$W = \sum_i \left[ \prod_{j=0}^{i-1} (1 - F_j) \right] F_i. \quad (24)$$

By using the model described above we have calculated the fissility for  $^{232}\text{Th}$  relative to  $^{238}\text{U}$ , and that for  $^{238}\text{U}$  and  $^{232}\text{Th}$  relative to  $^{237}\text{Np}$ . Although the multicollisional code, in its present version, is more accurate for energies above  $500\text{MeV}$ , we noticed that the relevant distributions of  $A_c$ ,  $Z_c$  and  $E_c$  for the compound nuclei are approximately independent of the incident photon energies in the intermediate energy range[14]. Therefore, we extended our model down to  $200\text{MeV}$  as the lower limit of our calculation.

In figure 1 we show the fissility for  $^{232}\text{Th}$  relative to  $^{238}\text{U}$ , and compare it with the data from Ref. [4]. We observe a striking agreement between our calculation and the experimental data, mainly above  $\sim 400\text{MeV}$ . The small deviation at lower energies may be attributed to the use of the multi collisional Monte Carlo at energies below its predicted limit of operation.

In figure 2 we show our results for the relative fissility for  $^{232}\text{Th}$  and  $^{238}\text{U}$  with respect to  $^{237}\text{Np}$ , and the experimental data to allow for a comparison. We observe that, as in the previous case, our results give a good description of the slowly varying behavior of the relative fissility for  $^{238}\text{U}$  and  $^{232}\text{Th}$  from  $200\text{MeV}$  to  $1000\text{MeV}$ , the approximate saturation being thus reproduced. Also, the absolute value is in good agreement with the data for both nuclei, with values ranging from  $\sim 0.45$  to  $\sim 0.60$  for  $^{232}\text{Th}$ , and from  $\sim 0.75$  to  $\sim 0.90$  for  $^{238}\text{U}$ .

These results show that our nuclear-evaporation/fission model, associated with the multicollisional Monte Carlo for the intranuclear cascade process, gives a good description for the photofissility data and clearly demonstrate the important role played by the proton and alpha particle emissions during the evaporation stage in the non-saturation of the photofissility. In fact, we performed the fissility calculations allowing only neutron evaporation, and the results, presented in Fig. 2, largely overestimate the experimental fissilities.



The absolute fissility is rather difficult to determine experimentally, since it depends on the measurement of two different quantities, namely, the total photoabsorption cross section and the photofission cross section. Even for those nuclei having both cross sections measured, the absolute fissility is uncertain due to the systematic errors in the experimental data from different laboratories which use different techniques.

However, at photon energies between 140 MeV and 1000 MeV these problems are partially overcome by the fact that the photoabsorption cross section is practically proportional to the nuclear mass number,  $A$  [4, 5, 6]. This allows the definition of a universal curve for the bound nucleon photoabsorption cross section,  $\sigma_{\gamma,a}(E)$ , which is related to the total nuclear photoabsorption cross section,  $\sigma_{\gamma,A}(E)$ , by

$$\sigma_{\gamma,A}(E) = \sigma_{\gamma,a}(E) A. \quad (25)$$

These quantities are related to the photofission cross section,  $\sigma_{\gamma,f}(E)$ , by

$$\sigma_{\gamma,f}(E) = A\sigma_{\gamma,a}(E)W. \quad (26)$$

The calculated fissility is shown in figure 3a, where we observe that  $W$  is higher than  $\sim 0.9$  for  $^{237}\text{Np}$  in the entire energy range, while saturating, at energies above  $400\text{MeV}$ , around  $W = 0.85$  for  $^{238}\text{U}$ , and, for  $^{232}\text{Th}$ , around  $W = 0.55$  only above  $500\text{MeV}$ .

By using eq. 26 we calculated the bound nucleon photoabsorption cross section for  $^{237}\text{Np}$ ,  $^{238}\text{U}$  and  $^{232}\text{Th}$ . The results, shown in figure 3b, are compared with the universal curve, which is composed of an upper and a lower limit for  $\sigma_{\gamma,a}$  obtained from the experimental photoabsorption cross sections for C, Al, Cu, Sn and Pb, using the photohadronic technique (see [26] and references therein). The agreement between the calculated photoabsorption cross sections and the universal curve is quite good, particularly above  $\sim 350\text{MeV}$ . Below this energy, our results overestimate the upper bound of the universal curve, probably due to the lower fissility values that we calculated. This behaviour is attributed to the fact that below  $350\text{MeV}$  we are considerably out of the  $500\text{MeV}$  limit for the intranuclear cascade algorithm used here.

Concluding, we have shown that the long-standing problem of the actinide nuclei fissility, which saturates at values smaller than 100% even at relatively high energies, can be understood from the combination of the MCMC model for the photon-induced intranuclear cascade process and our statistical model for the evaporation/fission process, which includes the evaporation of protons and alpha particles.

Besides shedding light on the photofissility issue, the present work could motivate the study of heavier actinides like e.g. americium and plutonium, in order to verify how their photofissilities respond to the emission of protons, alpha particles and also heavier clusters emissions (like lithium, boron, etc.), in both pre-equilibrium and evaporating stages. The former, in particular, is closely related to the important nuclear transparency issue (see e.g. the discussion presented in refs. [10] and [11]).

We acknowledge the support from the Brazilian agencies FAPESP and CNPq. One of the authors (A.D.) is thankful for the warm hospitality received during his stay at the CBPF.

## References

- [1] J. Ahrens et al., *Phys. Lett.* B146, 303 (1984).
- [2] A. Lepretre et al., *Nucl. Phys.* A472, 533 (1987).
- [3] A. S. Iljinov et al., *Nucl. Phys.* A539, 263 (1992).
- [4] N. Bianchi et al., *Phys. Rev.* C48, 1785 (1993).
- [5] N. Bianchi et al., *Phys. Lett.* B299, 219 (1993).
- [6] Th. Frommhold et al., *Phys. Lett.* B295, 28 (1992).
- [7] J. Ahrens, *Nucl. Phys.* A446, 229c (1985).
- [8] J. D. T. Arruda-Neto et al., *Phys. Lett.* B248, 34 (1990), and references therein.
- [9] G. J. Miller et al., *Nucl Phys* A551, 135 (1993).
- [10] J. D. T. Arruda-Neto et al., *Phys. Rev.* C51, 751 (1995).
- [11] A. Deppman et al.; *Nuovo Cimento* 109A, 1197 (1996).
- [12] J. C. Sanabria et al.; *Phys. Rev.* C61, 034604 (2000).
- [13] C. Cetina et al., *Phys. Rev. Lett.* 84, 5740 (2000).
- [14] M. Gonçalves et al.; *Phys. Lett* B406, 1 (1997).

- [15] V. Muccifora et al., Phys. Rev. C60, 064616 (1999).
- [16] H. W. Bertini; Phys. Rev. 131, 1801 (1963).
- [17] V. S. Barashenkov et al.; Nucl. Phys. A231, 462 (1974).
- [18] V. F. Weisskopf, Phys. Rev. 52, 295 (1937).
- [19] A. S. Iljinov, E. A. Cherepanov, and S. E. Chigrinov, Yad. Fiz. 32, 322 (1980) [Sov. J. Nucl. Phys. 32, 166 (1980)].
- [20] C. Guaraldo et al., Nuovo Cimento. 103A, 607 (1990).
- [21] N. Bohr and J. A. Wheeler, Phys. Rev. 56, 426 (1939).
- [22] R. Vandenbosch and J. R. Huizenga, Nuclear Fission, (1<sup>st</sup>ed., New York Academic Press, 1973) p227.
- [23] O. A. P. Tavares and M. L. Terranova, Z. Phys. A: Hadr. and Nucl. 343, 407 (1992).
- [24] K. J. LeCouteur, Proc. Phys. Soc. Lond., Ser. A63, 259 (1950).
- [25] E. Segrè, Nuclei and Particles, (3<sup>rd</sup>ed., W. A. Benjamin, INC, 1965) p215.
- [26] A. Deppman et al., Il Nuovo Cimento 111A, 1299 (1998).

## Figure Captions

**Figure 1:** Relative fissility for  $^{232}\text{Th}$  with respect to that for  $^{238}\text{U}$ . The full line is our present result, and the dotted lines show the upper and lower limits considering the 4% uncertainty associated with both the intranuclear cascade and nuclear evaporation/fission statistical evaluation. The experimental data are taken from Ref. [4].

**Figure 2:** Relative fissility for  $^{232}\text{Th}$  and  $^{238}\text{U}$  with respect to that for  $^{237}\text{Np}$ . Full and dotted lines have the same meaning as in fig.1. The experimental data are taken from Ref. [13]. The dashed and dash-dotted lines are the results of our calculations for  $^{232}\text{Th}$  and  $^{238}\text{U}$ , respectively, considering that only neutrons can be emitted during the evaporation/fission competition process.

**Figure 3:(a)** The nuclear calculated fissility as a function of the incident photon energy for  $^{237}\text{Np}$  (full line),  $^{238}\text{U}$  (dashed line) and  $^{232}\text{Th}$  (dotted line). **(b)** The bound nucleon photoabsorption cross section (see text), as a function of the incident photon energy, for  $^{237}\text{Np}$  (full circles),  $^{238}\text{U}$  (open circles) and  $^{232}\text{Th}$  (full squares). The full lines represent the upper and lower limits for the bound nucleon photoabsorption cross section, as can be deduced from the data reported in [26].

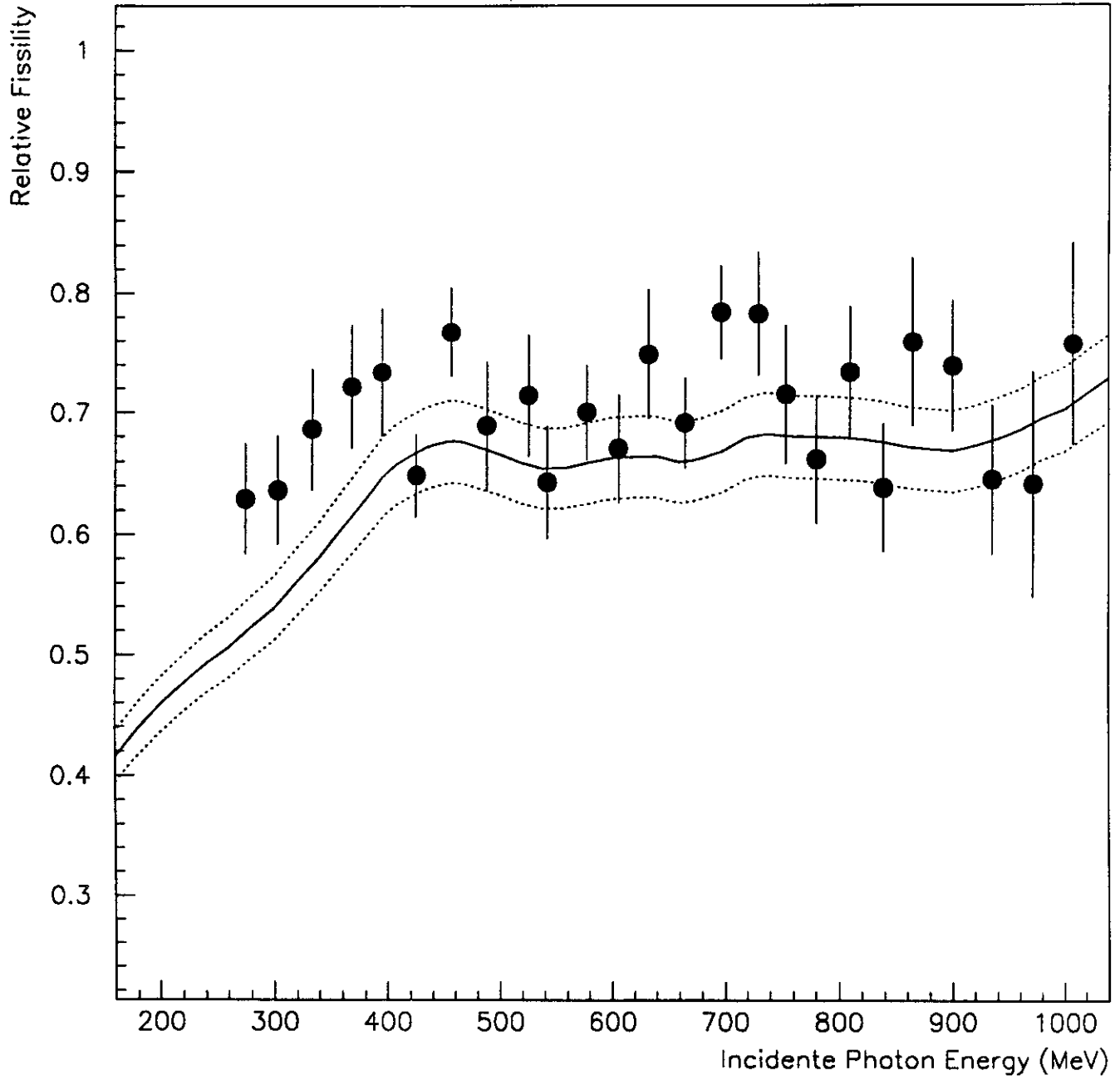


Figure 1

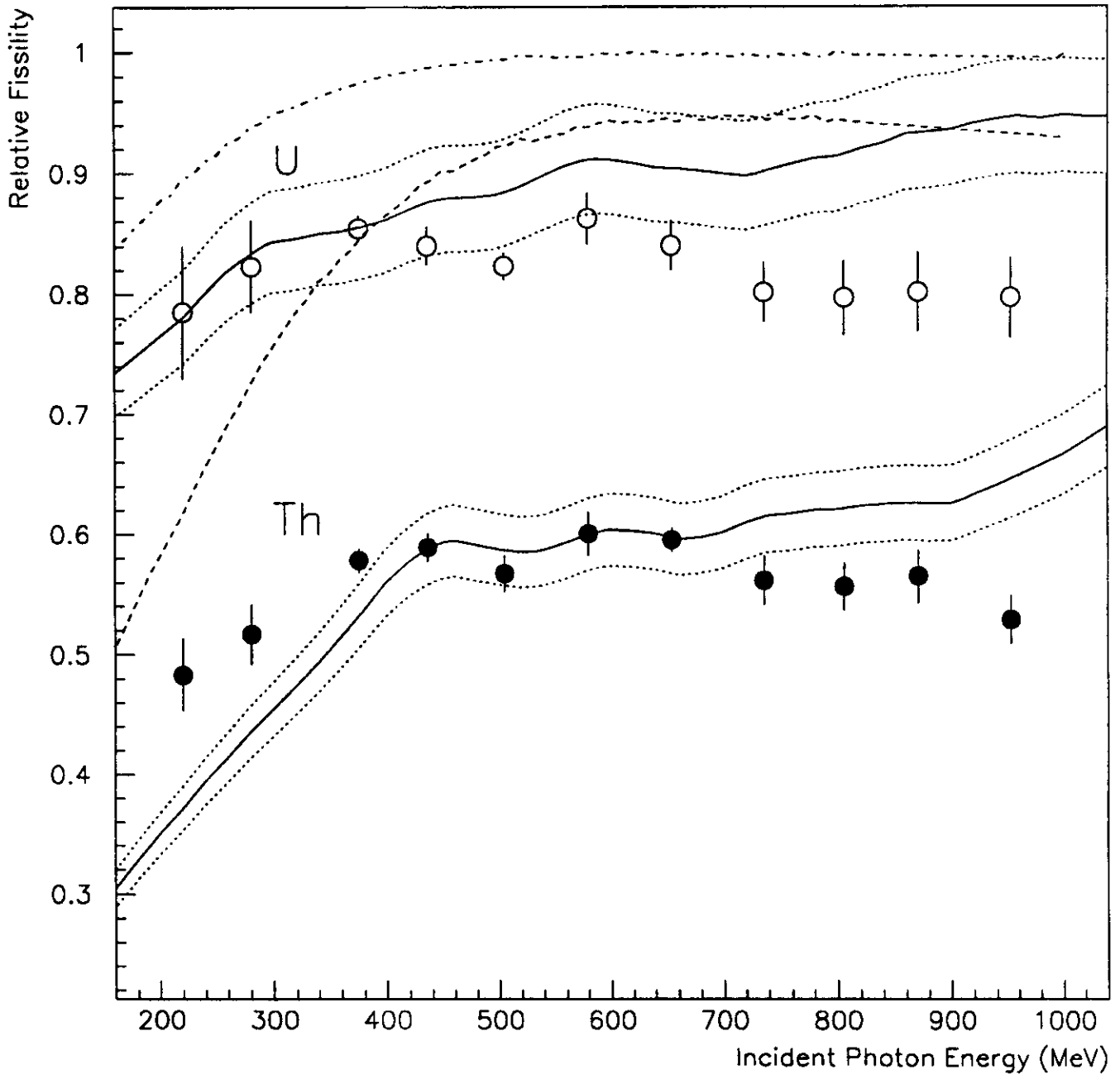


Figure 2

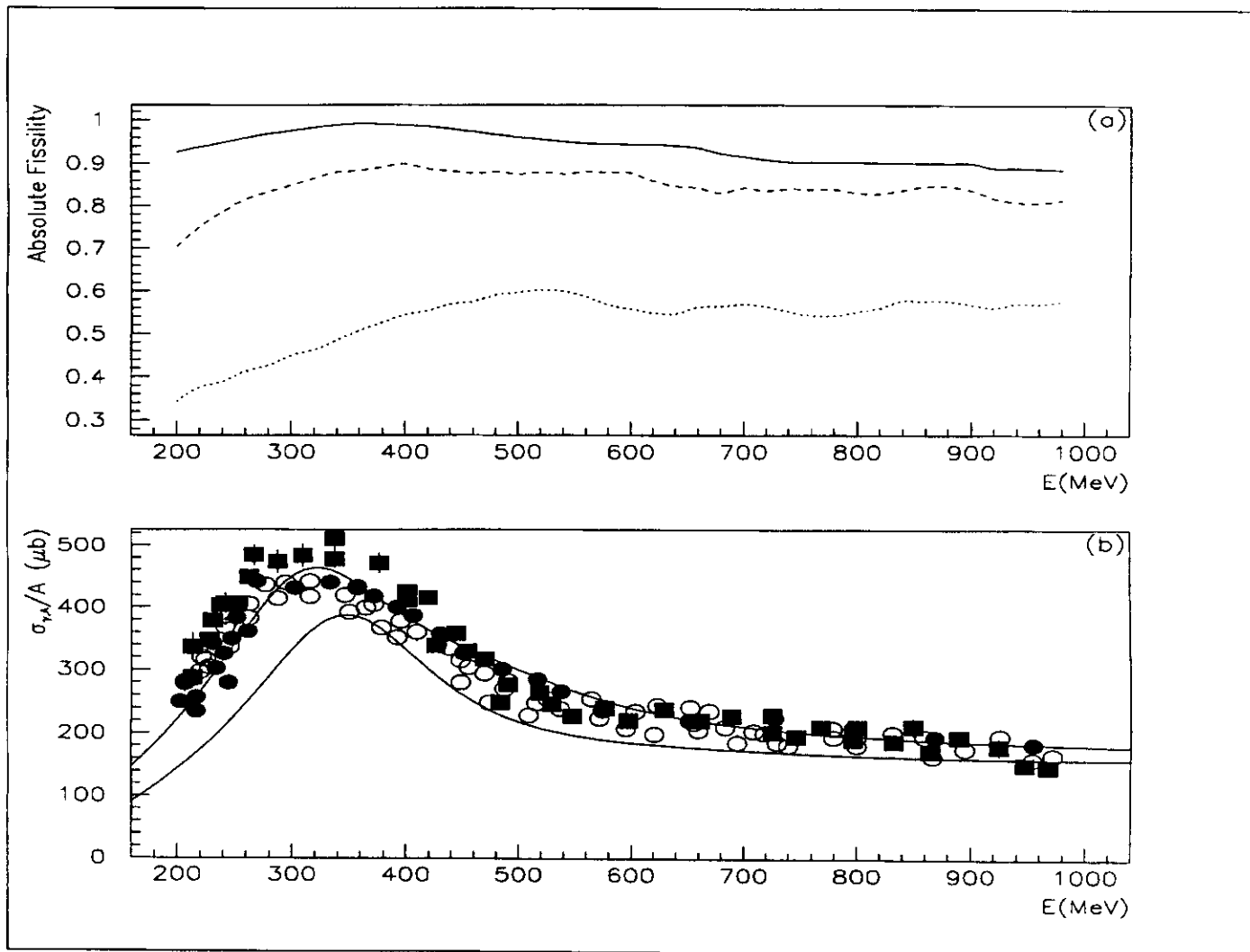


Figure 3

NOTAS DE FÍSICA é uma pré-publicação de trabalho original em Física.  
Pedidos de cópias desta publicação devem ser enviados aos autores ou ao:

Centro Brasileiro de Pesquisas Físicas  
Área de Publicações  
Rua Dr. Xavier Sigaud, 150 – 4<sup>o</sup> andar  
22290-180 – Rio de Janeiro, RJ  
Brasil  
E-mail: [socorro@cbpf.br](mailto:socorro@cbpf.br)/[valeria@cbpf.br](mailto:valeria@cbpf.br)

NOTAS DE FÍSICA is a preprint of original unpublished works in Physics.  
Requests for copies of these reports should be addressed to:

Centro Brasileiro de Pesquisas Físicas  
Área de Publicações  
Rua Dr. Xavier Sigaud, 150 – 4<sup>o</sup> andar  
22290-180 – Rio de Janeiro, RJ  
Brazil  
E-mail: [socorro@cbpf.br](mailto:socorro@cbpf.br)/[valeria@cbpf.br](mailto:valeria@cbpf.br)